XXII Congresso Brasileiro de Mecânica dos Solos e Engenharia Geotécnica
XI Simpósio Brasileiro de Engenheiros Geotécnicos Jovens
24 a 28 de agosto de 2026 – Brasília/DF
DOI: 10.47094/COBRAMSEG2026.4/102

Numerical Analysis of Unreinforced and Reinforced Embankment on Soft Soil using Geosynthetics and Encased Stone Columns

Naloan Coutinho Sampa
Professor, Federal University of Santa Catarina, Florianópolis, Brazil, naloan.sampa@ufsc.br

Jade Jacomini de Jesus
Master candidate, Federal University of Minas Gerais, Minas Gerais, Brazil, jade.jacomini@gmail.com

Bianca de Córdova Caetani
MSc., Federal University of Santa Catarina, Florianópolis, Brazil, bibicaetani@gmail.com

Gustavo Henrique Rossi
Civil Engineer, Federal University of Santa Catarina, Florianópolis, Brazil, gushenrirossi@hotmail.com

ABSTRACT: Soft clay foundations challenge embankment performance due to high compressibility and coupled hydro-mechanical response. This study presents fully coupled two-dimensional finite element analyses in Abaqus/Standard comparing unreinforced, basal geosynthetic-reinforced, and geosynthetic-encased stone column (GEC) foundations. The clay was modeled using Modified Cam Clay with staged construction and consolidation. A parametric study examined the influence of clay thickness, overconsolidation ratio (OCR), recompression index (κ), critical state parameter (M), geosynthetic stiffness (J), column spacing ratio (s/d), and column modulus (E_c). In unreinforced and geosynthetic-reinforced systems, settlement is governed by clay compressibility, while basal reinforcement mainly reduces lateral displacement (up to 35%) with limited settlement reduction (≈4%). GECs alter load transfer through stiffness contrast and soil arching, reducing settlement by ≈30% and accelerating consolidation. Settlement reduction increases systematically with stiffness contrast (E_c/E_s) and area replacement ratio. The results define distinct vertical and lateral improvement mechanisms and provide quantitative criteria for optimized embankment design on soft clay.

Keywords: Finite element analysis, Modified Cam Clay, Abaqus, Consolidation, Coupled consolidation.

1 INTRODUCTION

The construction of embankments on soft, saturated clays remains one of the most critical challenges in geotechnical engineering. The difficulty arises from strongly coupled hydro-mechanical processes: applied loading induces large deformations and excess pore pressures, whose subsequent dissipation alters the effective stress state and governs settlement development. Soft clays are characterized by low undrained shear strength, high compressibility, and low permeability. These characteristics lead to significant vertical settlements, lateral spreading, and potential instability during staged construction, as both short-term stability and long-term performance are controlled by stress redistribution and time-dependent consolidation.

Classical consolidation theory (Terzaghi, 1925; Terzaghi and Fröhlich, 1936) established the theoretical framework for predicting primary settlement through pore pressure dissipation. However, embankment behavior on soft clay involves nonlinear stress-strain response, volumetric hardening, and stress-path dependency. These mechanisms cannot be adequately represented by traditional rigid-plastic or limit equilibrium approaches (Duncan and Wright, 2005), which neglect progressive deformation and hydro-mechanical coupling.

The Finite Element Method (FEM) provides a consistent framework to address these limitations. Coupled consolidation formulations enable simulation of staged construction and transient pore pressure evolution (Zienkiewicz and Taylor, 2000). When integrated with advanced constitutive models such as

Modified Cam Clay (Roscoe and Burland, 1968; Wood, 1990), FEM captures stress-dependent stiffness, overconsolidation effects, and volumetric hardening. These features are essential for realistic prediction of settlements and lateral displacements in soft foundations.

To control excessive deformation and improve stability, ground improvement techniques are frequently adopted. Basal geosynthetic reinforcement enhances performance through tensile membrane action, which restrains lateral spreading and redistributes loads within the embankment-foundation system (Rowe and Soderman, 1986; Bonaparte and Christopher, 1987). Its effectiveness depends primarily on tensile stiffness and anchorage conditions. Stone columns constitute an alternative strategy. They increase composite stiffness and accelerate consolidation through radial drainage (Balaam and Booker, 1981; Castro and Sagaseta, 2011). Despite these benefits, in very soft soils, conventional stone columns may experience excessive bulging due to insufficient lateral confinement (Hughes and Withers, 1974). Geosynthetic-encased stone columns (GECs) mitigate this limitation by mobilizing hoop tensile stresses within the encasement, thereby improving confinement, load transfer efficiency, and deformation control (Alexiew et al., 2005; Murugesan and Rajagopal, 2010).

Although these techniques have been extensively studied individually, systematic comparative analyses conducted within a unified, fully coupled numerical framework remain limited. In particular, the combined influence of soil constitutive parameters - such as overconsolidation ratio (OCR), recompression index (κ), and critical state parameter (M) - and reinforcement parameters - such as tensile stiffness (J), column spacing ratio (s/d), and stiffness contrast (E_c/E_s) - has not been quantified in a consistent manner. This limitation restricts the development of optimized and mechanistically informed design strategies.

This study addresses this gap through a rigorous two-dimensional finite element investigation performed in Abaqus/Standard. Three configurations are analyzed within a consistent modeling framework: (i) unreinforced embankment, (ii) embankment with basal geosynthetic reinforcement, and (iii) foundation improved with geosynthetic-encased stone columns. Staged construction and fully coupled consolidation are simulated to capture the time-dependent evolution of settlements and lateral displacements.

A comprehensive parametric study evaluates the influence of clay layer thickness, OCR, κ, M, J, s/d, and E_c/E_s. The findings clarify the interaction between tensile membrane action and composite stiffness effects, providing a rational and mechanistically consistent basis for the optimized design of reinforced embankments on soft clay deposits.

2 FINITE ELEMENT MODEL

Numerical analyses were performed using Abaqus/Standard to investigate the hydro-mechanical response of embankments constructed on soft clay. Three configurations were considered: (i) unreinforced embankment, (ii) embankment with basal geosynthetic reinforcement, and (iii) foundation improved with geosynthetic-encased stone columns (GECs). Owing to symmetry, only half of the embankment–foundation system was modeled.

2.1 Geometry, Construction Sequence, and Boundary Conditions

The reference embankment is 3.5 m high, with 1V:2H side slopes and a 20 m crest width. It is founded on a 10 m thick clay layer extending 60 m horizontally. The domain dimensions were verified to prevent boundary influence within the zone of interest.

Fully coupled stress-pore pressure analyses were conducted to simulate consolidation. The numerical procedure comprised three stages: i) a geostatic step to establish initial effective stresses and a hydrostatic pore pressure distribution; ii) staged embankment construction over one month using linear load incrementation; iii) a four-year consolidation phase.

During initialization, zero pore pressure was imposed at the ground surface. After construction, free-drainage conditions were applied along exposed boundaries. The model base was fully restrained. Horizontal displacements were restricted along vertical boundaries, and symmetry conditions were enforced along the centerline.

2.2 Discretization and Constitutive Modeling

The finite element mesh is shown in Figure 1. Plane strain simulations employed eight-node quadrilateral elements with reduced integration and pore pressure degrees of freedom (CPE8RP). Axisymmetric analyses of the column-reinforced configuration used CAX8RP elements. Mesh refinement was concentrated beneath the embankment and around column inclusions to accurately capture stress and strain gradients.

The soft clay was modeled using the Extended Modified Cam Clay formulation. This model represents stress-dependent stiffness, volumetric hardening, and consolidation behavior. The embankment fill and granular columns were described using Mohr-Coulomb model.

Reference material parameters and their variation ranges are summarized in Table 1. Parameter values were selected based on representative experimental and numerical studies reported in the literature (See Caetani, 2022; De Jesus, 2022 and Rossi, 2022).

The geosynthetic reinforcement was modeled using B22 beam elements. Its mechanical behavior was defined by axial stiffness (J), thickness, and Poisson's ratio, as summarized in Table 2.

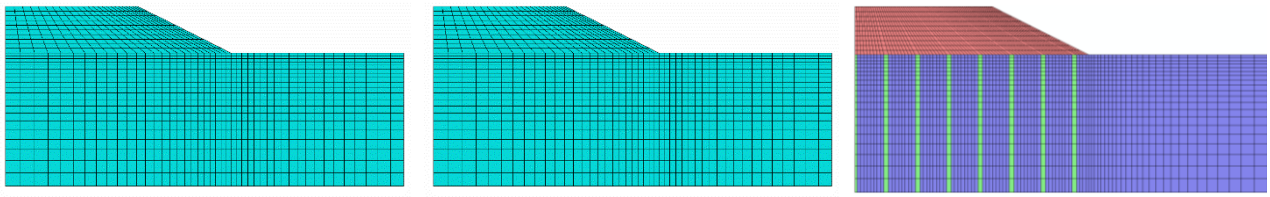


Figure 1. Representation of discretized finite element domain and boundary conditions.

Table 1. Parameters of the soft soil and granular material of embankment.

	Soft Soil		Granular material - embankment		Granular material - column	
Parameter	Reference values	Variation range	Reference values	Variation range	Reference values	Variation range
e_0	1.2	1 - 2	0.65	-	0.72	-
γ (kN/m³)	15	14 - 18	20	18 - 22	20	19 - 23
κ	0.05	0.03 – 0.09	-	-		
ν	0.33	0.35 – 0.45	0.3	0.3 – 0.35	0.3	0.2 – 0.35
λ	0.2	0.11 – 0.5	-	-	-	-
M	1	0.85 – 1.4	-	-	-	-
p'/σ'_{v0}	37.5	-	-	-	-	-
β	1	-	-	-	-	-
K	1	-	-	-	1E-05	-
k (m/s)	2.50E-08	-	0.01	-		
$K_0 = 1 - \text{sen}\,\phi$	0.58	0.58 – 0.66				0.318
c (kN/m²)	-	-	2	0 - 5	1	0 - 1
ϕ (°)	-	-	30	25 - 40	43	33 - 45
ψ (°)	-	-	10	0 - 10	5	2.5 - 10
E (kN/m²)	-	-	1000	500 - 80000	30	14 - 40

Table 2. Parameters of geosynthetics.

Parameter	Reference values	Variation range
layers – n	1.0	0 a 4.0
Poisson's ratio – υ	0.15	0 a 0.45
Thickness – t (mm)	3.0	-
Modulus of rigidity – J (kN/m)	3000	1000 a 5000

2.3 Modeling of Reinforcement Configurations

The baseline configuration included only embankment fill and soft clay. Nineteen simulations were performed to evaluate the influence of clay thickness (H_s of 5, 10, 15 and 20 m) and key clay parameters on settlement and lateral displacement. This configuration serves as the reference for assessing improvement efficiency. Additional insights into these simulations are available in Caetani (2022).

Basal reinforcement was modeled by placing B22 beam elements at the embankment. The reinforcement was activated during construction. Soil-reinforcement interaction was governed by displacement compatibility, allowing tensile forces to develop in response to lateral spreading.

The parametric study considered one to four reinforcement layers and tensile stiffness values ranging from 1000 to 5000 kN/m. A total of 48 simulations were conducted to quantify the influence of stiffness and layer number on global response and reinforcement demand. Additional insights into these simulations are available in Rossi (2022).

Stone columns extended through the full clay thickness. Two complementary modeling approaches were adopted. In plane strain, columns were represented as continuous walls with equivalent thickness calculated to preserve the area replacement ratio, following the transformation proposed by Van Impe and De Beer (1983). In axisymmetric analyses, a unit-cell model was employed to capture three-dimensional confinement and radial drainage effects. Full displacement compatibility at the soil-column interface was assumed using tied contact.

A total of 96 simulations were performed (48 plane strain and 48 axisymmetric), varying column spacing ratio (s/d) and column elastic modulus (E_c) to evaluate their influence on settlement reduction and stress redistribution. Additional insights into these simulations are available in De Jesus (2022).

2.4 Response Evaluation

Embankment performance was evaluated in terms of crest settlement, foundation settlement, and lateral displacement. For reinforced configurations, tensile forces and strains in the geosynthetic layers were additionally monitored. Monitoring points and extraction sections (Figure 2) were defined to enable consistent spatial and temporal comparison across all configurations and parametric cases.

Embankment performance was assessed in terms of crest settlement, foundation surface settlement, and lateral displacement.

For reinforced configurations, tensile forces and strains in the geosynthetic layers were additionally monitored.

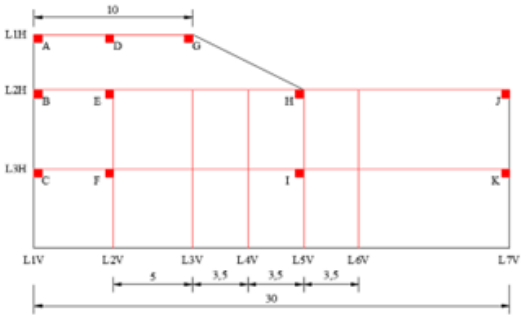


Figure 2. Points and lines used to extract the data.

3 RESULTS AND DISCUSSION

This section synthesizes the results of all fully coupled finite element simulations. The influence of clay thickness (H_s), overconsolidation ratio (OCR), swelling index (κ), critical state parameter (M), and reinforcement parameters is evaluated in terms of settlement and horizontal displacement. Only representative cases are presented; however, the observed trends were consistent across all parametric combinations.

3.1 Settlement Analysis

Settlement behavior was evaluated in terms of magnitude, temporal evolution and horizontal for the unreinforced, geosynthetic-reinforced, and stone column–reinforced configurations. All normalized settlements are expressed relative to the soft clay thickness H_s =10 m unless otherwise stated. Figure 3 illustrates the spatial distribution of settlement at the end of embankment after the consolidation phase (48 months).

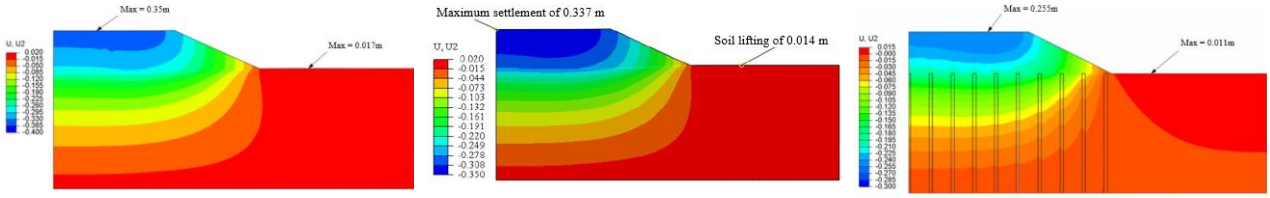


Figure 3. a) unreinforced embankment; b) embankment reinforced with geosynthetic; c) improvement with encased stone columns.

3.1.1 *Unreinforced Embankment*

For the unreinforced reference case (H_s = 10 m), crest settlement reached 35 cm (3.5% H_s) after consolidation. Approximately 70% developed during the one-month construction stage, confirming the dominance of the undrained response during loading. Primary consolidation was essentially complete after 12-14 months.

A transient toe uplift of 9 cm occurred during construction due to rapid lateral spreading. This reduced to 2 cm after consolidation (Figure 4), reflecting stress redistribution toward the crest.

Increasing clay thickness from 5 m to 20 m increased absolute settlement (ρ) (26-42.4 cm) but reduced normalized settlement (ρ/H_s) (4.0%-2.1%). This reflects lower average vertical strain in thicker deposits under identical loading.

Parametric analysis confirms that settlement is governed primarily by clay compressibility. The recompression index (κ) exerts the strongest influence ($\uparrow\ \kappa \rightarrow \uparrow\ \rho/H_s$), while the critical state parameter (M) produces a consistent but secondary increase ($\uparrow\ M \rightarrow \uparrow\ \rho/H_s$). Embankment properties (φ, E) and clay compression index (λ) have negligible influence within the investigated ranges, demonstrating that vertical deformation is controlled by foundation stiffness rather than fill characteristics.

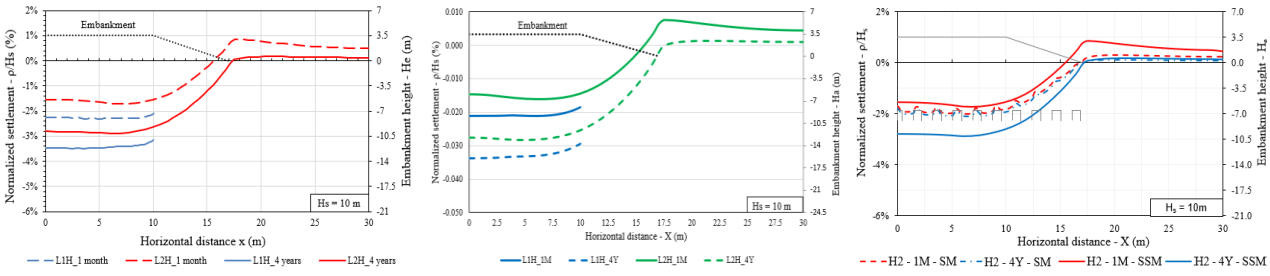


Figure 4. Variation of the settlement versus horizontal distance – a) unreinforced embankment; b) embankment reinforced with geosynthetic; c) improvement with encased stone columns.

3.1.2 *Geosynthetic-Reinforced Embankment*

The inclusion of a single basal geosynthetic layer reduced crest settlement to 33.7 cm, corresponding to a modest reduction of approximately 4%. The temporal evolution remained nearly identical to the unreinforced case.

Variations in tensile stiffness (J = 1000 - 5000 kN/m) and number of layers (n = 1 - 4), embankment modulus (E), and geosynthetic Poisson's ratio (ν) had negligible influence on settlement magnitude. Settlement curves were nearly coincident once a minimum stiffness threshold was exceeded. This confirms

that vertical compression is governed by clay compressibility rather than reinforcement stiffness.

Toe uplift was reduced to 5 - 7 cm during construction and to 1.4 - 2 cm after the total consolidation. However, deformation below $z/H_s \approx 0.7$ remained comparable to the unreinforced case. Basal geosynthetics therefore function primarily as near-surface tensile restraint systems and do not significantly modify vertical stress transfer or drainage conditions.

3.1.3 *Stone Column–Reinforced Embankment*

Geosynthetic-encased stone columns (GECs) significantly modified both settlement magnitude and rate. Crest settlement was reduced to 25-26 cm, corresponding to a reduction of approximately 28-30%. Settlement at the clay surface exhibited similar reductions.

Unlike the geosynthetic case, the improved foundation stabilized almost immediately after construction. Although short-term settlement remained comparable to the unreinforced system due to stress concentration in the stiff inclusions, accelerated drainage and enhanced composite stiffness effectively limited long-term settlement growth.

Settlement profiles exhibited oscillatory patterns associated with stiffness contrast. Settlements directly above columns were approximately 5 cm lower than in adjacent soil zones, confirming effective load transfer through soil arching and stress concentration in the inclusions.

Column efficiency was quantified using the settlement reduction factor: $\beta = \rho_{\text{unreinforced}}/\rho_{\text{reinforced}}$. During construction, $\beta \approx 1$ due to stress concentration effects. After approximately eight months, β exceeded unity as consolidation progressed in the unreinforced system. After the end of consolidation, β ranged between 1.30 and 1.40, indicating long-term settlement reductions of nearly one-third.

Parametric results demonstrate that β increases approximately linearly with stiffness contrast (E_c/E_s) and area replacement ratio (a_c). Within the investigated range, β increased from 1.2 to 1.8 as a_c increased from 0.10 to 0.25, demonstrating the direct and predictable benefit of increased inclusion density. When ac was held constant, increasing column diameter generated competing effects between individual column stiffness and load-transfer density. This confirms that the replacement ratio, rather than column diameter alone, governs settlement control.

Overall, settlement behavior is controlled by clay compressibility in unreinforced and geosynthetic-reinforced systems, whereas in column-reinforced systems it is governed by composite stiffness and stiffness contrast. Geosynthetics provide limited influence on vertical response, while stone columns fundamentally modify load transfer and drainage conditions.

3.2 Horizontal Displacement

3.2.1 *Unreinforced Embankment*

Figure 5 shows the spatial distribution of horizontal displacement (δ_h), at 12 months. Maximum horizontal displacement occurred beneath the embankment toe, reaching 18 cm during construction and reduced to 14 cm after consolidation. This 22% reduction reflects stress redistribution during consolidation. Stabilization occurred after approximately one year.

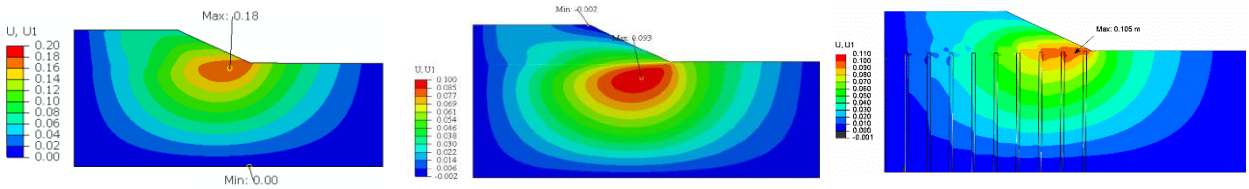


Figure 5. 1 year – a) unreinforced embankment; b) embankment reinforced with geosynthetic; c) improvement with encased stone columns.

A non-monotonic trend was observed: normalized horizontal displacement (δ_h/H_e) increased as clay thickness increased from 5 m to 10 m, followed by a decrease for thicknesses up to 20 m. The swelling index

(κ) strongly increased lateral displacement, while higher friction angle (φ) reduced it slightly through enhanced shear strength. The critical state parameter (M) and elastic modulus (E) produced moderate increases of lateral displacement.

3.2.2 *Geosynthetic Reinforcement*

In contrast to settlement behavior, horizontal displacement was highly sensitive to reinforcement properties. Figure 6 presents the typical variation of δ_h/H_e along z/H_s for different vertical lines (LV). Peak displacement reduced to 14 cm during construction and 9 cm after four years, corresponding to a long-term reduction of approximately 35%.

Increasing tensile stiffness (J) and number of layers (n) reduced displacement nonlinearly. A reduction plateau is expected for larger n and J, indicating a transition from reinforcement-controlled to soil-controlled behavior once tensile membrane action was fully mobilized. Embankment modulus (E) has minor long-term influence ($\uparrow E \rightarrow \uparrow \delta_h/H_s$), and geosynthetic Poisson's ratio (ν) remains negligible.

The reduction was concentrated in the upper clay layer ($z/H_s < 0.7$). Deeper deformation patterns remained similar to the unreinforced case, confirming that geosynthetics act primarily as near-surface tensile restraint systems without significantly altering deeper stress redistribution.

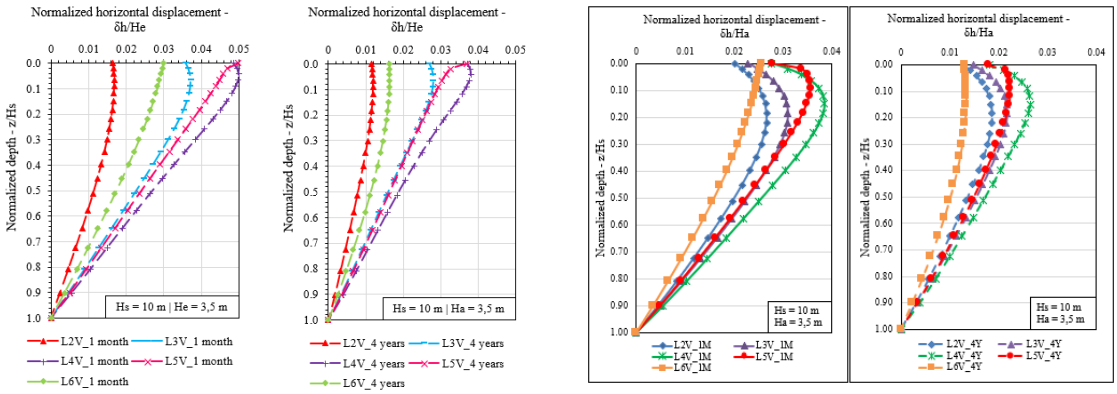


Figure 6. Variation of the horizontal displacement along the depth – a) unreinforced embankment; b) embankment reinforced with geosynthetic.

3.2.3 *Stone Columns*

Stone columns reduced peak horizontal displacement by approximately 22% and significantly limited deformation propagation. Lateral movement became more localized and decreased progressively with depth.

Increasing stiffness contrast (E_c/E_s) and replacement ratio (a_c) reduced displacement magnitude. Sensitivity to column diameter was secondary, reflecting its indirect influence through stiffness contrast. Columns located beneath the slope exhibited the greatest benefit, consistent with local shear stress concentration.

The difference between plane strain and axisymmetric analyses remained below 5%, confirming the robustness of the equivalent transformation adopted for two-dimensional modeling.

Horizontal displacement is governed by shear strength and compressibility in the unreinforced system. Geosynthetics reduce lateral spreading through tensile membrane action concentrated near the surface, whereas stone columns act through composite stiffness enhancement and stress redistribution. Thus, vertical and lateral responses are controlled by distinct mechanisms, and improvement strategies must be selected according to the governing performance criterion.

4 CONCLUSIONS

This study compared unreinforced, geosynthetic-reinforced, and GEC-improved embankments on soft clay using fully coupled finite element analyses. The main findings are:

- Unreinforced embankments: Settlement is governed by clay compressibility (κ dominant). Approximately 70% of final settlement occurs during construction.
- Basal geosynthetics: Lateral displacement decreases up to 35% through membrane action, whereas settlement reduction is marginal (≈4%) and independent of stiffness.
- GECs: Settlement decreases by 28–30% and consolidation accelerates due to enhanced composite stiffness and radial drainage. Lateral displacement reduces by ≈22%.
- Design parameters: The settlement reduction factor (β) increases linearly with stiffness contrast (E_c/E_s) and area replacement ratio (a_c), ranging from 1.2 to 1.8 for ac = 0.10–0.25. Replacement ratio governs settlement control more than column diameter.
- Mechanisms: Geosynthetics provide near-surface tensile restraint; GECs modify load transfer through stress concentration and soil arching.

In practice, geosynthetics address stability, whereas GECs provide comprehensive serviceability improvement. Technique selection should follow the governing performance requirement.

REFERENCES

Alexiew, D., Brokemper, D., Lothspeich, S. (2005). Geotextile encased columns (GEC): Load capacity, geotextile selection and pre-design graphs. In: Proceedings of the International Symposium on Ground Improvement, Brussels.

Balaam, N. P., Booker, J. R. (1981). Analysis of rigid rafts supported by granular piles. International Journal for Numerical and Analytical Methods in Geomechanics, v. 5, n. 4, p. 379–403.

Bonaparte, R., Christopher, B. R. (1987). Design and construction of reinforced embankments over weak foundations. Transportation Research Record, n. 1153, p. 26–39.

Caetani, Bianca de Córdova (2022). Simulação numérica e análise paramétrica do comportamento de um aterro sobre solos moles. 2022. 147 f. TCC (Graduação) - Curso de Engenharia Civil, Centro Tecnológico, Universidade Federal de Santa Catarina, Florianópolis, 2022.

Castro, J., Sagaseta, C. (2011). Consolidation around stone columns: Influence of column deformation. International Journal for Numerical and Analytical Methods in Geomechanics, v. 35, n. 7, p. 831–847.

Duncan, J. M., Wright, S. G. (2005). Soil Strength and Slope Stability. Hoboken: John Wiley & Sons.

Hughes, J. M. O., Withers, N. J. (1974). Reinforcing of soft cohesive soils with stone columns. Ground Engineering, v. 7, n. 3, p. 42–49.

De Jesus, Jade Jacomini (2022). Desempenho de aterro sobre solo mole melhorado pela técnica de colunas granulares: simulação numérica e análise paramétrica. 2022. 166 f. TCC (Graduação) - Curso de Engenharia Civil, Centro Tecnológico, Universidade Federal de Santa Catarina, Florianópolis, 2022

Murugesan, S., Rajagopal, K. (2010). Studies on the behavior of single and group of geosynthetic encased stone columns. Journal of Geotechnical and Geoenvironmental Engineering, v. 136, n. 1, p. 129–139.

Roscoe, K. H., Burland, J. B. (1968). On the generalized stress–strain behaviour of "wet" clay. In: Heyman, J.; Leckie, F. A. (eds.). Engineering Plasticity. Cambridge: Cambridge University Press, p. 535–609.

Rossi, Gustavo Henrique (2022). Estudo do comportamento de aterros reforçados com geossintéticos sobre solos moles: simulação numérica e análise paramétrica. 2022. 124 f. TCC (Graduação) - Curso de Engenharia Civil, Centro Tecnológico, Universidade Federal de Santa Catarina, Florianópolis, 2022.

Rowe, R. K., Soderman, K. L. (1986). Stabilization of very soft soils using high strength geosynthetics: The role of finite element analysis. Canadian Geotechnical Journal, v. 23, n. 4, p. 484–497.

Terzaghi, K. (1925). Erdbaumechanik auf bodenphysikalischer Grundlage. Wien: Franz Deuticke.

Terzaghi, K., Fröhlich, O. K. (1936). Theorie der Setzung von Tonschichten. Wien: Franz Deuticke.

Van Impe, W. and De Beer, E. (1983). Improvement o f Settlement Behaviour o f Soft Layers by means of Stone Columns. Proc. 8th Euro. Conf. on Soil Mech.A Fdn. Engg., Helsinki, 1983. P. 309-312.

Wood, D. M. (1990). Soil Behaviour and Critical State Soil Mechanics. Cambridge: Cambridge University Press.

Zienkiewicz, O. C., Taylor, R. L. (2000). The Finite Element Method. Volume 2: Solid Mechanics. 5. ed. Oxford: Butterworth-Heinemann.